JOURNAL OF NANO- AND ELECTRONIC PHYSICS
Vol. **5** No 1, 01007(4pp) (2013)

ЖУРНАЛ НАНО- ТА ЕЛЕКТРОННОЇ ФІЗИКИ
Том **5** № 1, 01007(4cc) (2013)

Luminescence Properties of Ce^{3+}-Doped Terbium Aluminum Garnet Phosphor Prepared with Use of Nanostructured Reagents

I.V. Berezovskaya[1,*], B.I. Zadneprovski[2], N.I. Poletaev[3], Yu.A. Doroshenko[3], N.P. Efryushina[1], E.V. Zubar[1], V.P. Dotsenko[1]

[1] *A.V. Bogatsky Physico-Chemical Institute, National Academy of Sciences of Ukraine, 86, Lustdorfskaya doroga, 65080 Odessa, Ukraine*
[2] *Central Research and Development Institute of Chemistry and Mechanics, 115487 Moscow, Russia*
[3] *Institute of Combustion and Advanced Technologies, Mechnikov Odessa National University, 2, Dvoryanskaya str., 65082 Odessa, Ukraine*

(Received 07 November 2012; revised manuscript received 15 December 2012; published online 28 March 2013)

The paper describes the synthesis of Ce^{3+}-doped terbium aluminum garnet (TAG) phosphors with use of nanostructured oxides of aluminum and rare earths. Aluminum oxide nanoparticles were obtained by gaseous-disperse synthesis and characterized by X-ray diffraction, differential thermal analysis and scanning electron microscopy. It was shown that the Ce^{3+} ions in TAG exhibit the intense broad band emission with a maximum at about 563 nm and the quantum efficiency of luminescence of the $Tb_{3(1-x)}Ce_{3x}Al_5O_{12}$ ($x = 0.03$) phosphor was found as high as 0.83.

Keywords: Terbium Aluminum Garnet, Synthesis, Nanopowders, Luminescence.

PACS numbers: 78.47.jd, 81.07.Wx

1. INTRODUCTION

The white light-emitting diodes (LED's) are one of the most promising alternatives to conventional electric light sources, i.e. incandescent lamps, Hg-containing fluorescent lamps. This concept has been commercially realized by using a combination of a blue LED emitting around 460 nm and yttrium aluminum garnet ($Y_3Al_5O_{12}$, YAG) doped with Ce^{3+} ions as a yellow phosphor. The restricting factor in using such white LED's for general lighting is a low color rendering index ($R_a < 80$) that is caused by a deficit of red component in the emission spectrum of YAG:Ce^{3+} [1, 2]. The shortcomings of YAG:Ce^{3+}-based white LED's stimulated the search for alternative compositions with the garnet structure [1, 2] and, in particularly, the attempts to improve the color characteristics of LED's by substitution of Y^{3+} with other rare earth (R) ions. Jang et al. [3] have studied the luminescent properties of Ce^{3+} ions in $Tb_{3x}Y_{3(1-x)}Al_5O_{12}$ (TYAG) solid solutions. It was found that the Tb^{3+} substitution induces larger crystal field splitting of the Ce^{3+} 5*d* configuration and shifts the Ce^{3+} emission band towards longer wavelengths. Since this emission is efficiently excited by photons in the 380-460 nm region, efficient white LED's were fabricated by using a combination of (In, Ga)N chips emitting around 460 nm and TYAG:Ce^{3+} as a yellow-orange phosphor. Also, several groups of authors have studied the luminescent properties of Ce^{3+} ions in $Tb_3Al_5O_{12}$ (TAG) upon excitation in the 240-550 nm region [4-6]. It was shown that there is an efficient energy transfer between Tb^{3+} and Ce^{3+} in TAG and this material can be also of interest for development of new scintillators [5]. As a rule, Ce-containing garnets phosphors are prepared by solid state reactions between starting reagents at temperatures, which typically exceed 1500 °C.

Even then, depending upon the preparation conditions some amounts of impurity phases such as $RAlO_3$, CeO_2 can be revealed in the final products [2, 7]. Besides, an insufficient mixing and low reactivity of raw materials often result in the significant difference in the Ce^{3+} concentrations within the grains and in the vicinity of grain boundaries [8]. In the present paper, we describe the synthesis of $Tb_{3(1-x)}Ce_{3x}Al_5O_{12}$ ($x = 0$-0.03) luminescent materials by solid state reactions between aluminum oxide Al_2O_3 and mixed rare earth oxides. Our approach included the use of a nanosized metastable Al_2O_3, the use of oxalate precursor-derived rare earth oxides, the firing of reaction mixtures in the temperature region of a metastable alumina phase to α-Al_2O_3 transition. It was expected that an acceleration of the diffusion of Al^{3+} and O^{2-} in temperature region of the Al_2O_3 phase transformation would stimulate the solid state reactions. The results of luminescent measurements on the obtained materials are also reported and discussed.

2. EXPERIMENTAL

All samples were characterized by X-ray diffraction (XRD) using Cu K_α radiation (Rigaku Ultima IV). Differential thermal analysis (DTA) was performed on a thermal analyzer (LABSYS DSC/DTA/TG) in air at a heating rate of 20 °C/min. Morphological investigations were carried out by scanning electron microscopy (SEM) on JEOL JSM 6390LV electron microscope. The particle size distribution of nanosized Al_2O_3 was obtained by laser diffraction method using a Shimadzu SALD 2201 analyzer. The emission and excitation spectra in UV-visible region were recorded at 77 K and room temperature using a Fluorolog Fl-3 (Horiba Jobin Yvon) spectrofluorometer equipped with a xenon lamp.

* ssclab@ukr.net
The article was reported at the 2nd International Conference «Nanomaterials: Applications & Properties-2012»

3. RESULTS AND DISCUSSION

Nanosized Al_2O_3 was obtained by a gaseous-disperse synthesis. This method is based on the combustion of powdered metals due to exothermic oxidizing reactions between them and a gaseous oxidizer (typically O_2). The details of experimental setup used for the synthesis of nanosized Al_2O_3 can be found in the paper by Poletaev et al. [9]. The dispersed in N_2 aluminum particles with an average size of 4.8 μm were injected through an inner tube into O_2 stream. After ignition by an external source, a stable two-phase diffusion flame was observed. The resulting product was collected using a fabric filter. The XRD pattern of the as-prepared Al_2O_3, shown in Fig. 1, indicates that the powder contains γ,δ,θ-phases of Al_2O_3, which are present in approximately the same quantities.

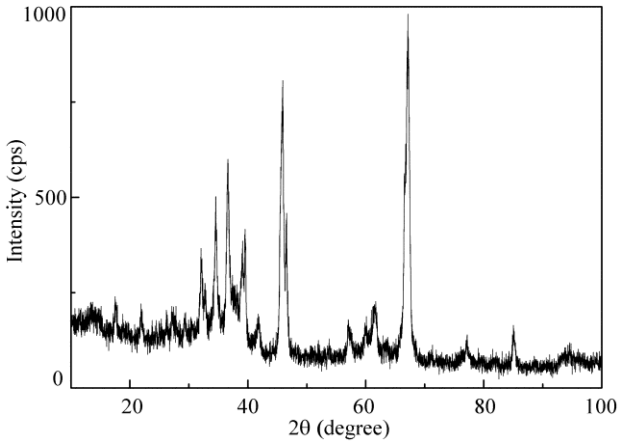

Fig. 1 – Powder X-ray diffraction pattern of as-prepared Al_2O_3

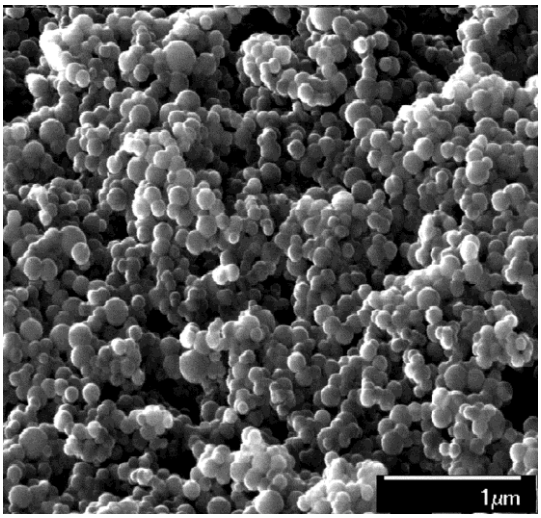

Fig. 2 – SEM photograph of as-prepared Al_2O_3

As can be seen from Fig. 2, its crystallites are of spherical in shape with 20-70 nm in diameter, and they exhibit a tendency to adhesion. Fig. 3 shows the particle size distribution of the as-prepared Al_2O_3. It is seen that the size of majority of the particles does not exceed 70 nm and the average size of crystallites was found to be ~ 49 nm. Probably, due to the size limitations of the analyzer used in this study this value somewhat exceeds the real one.

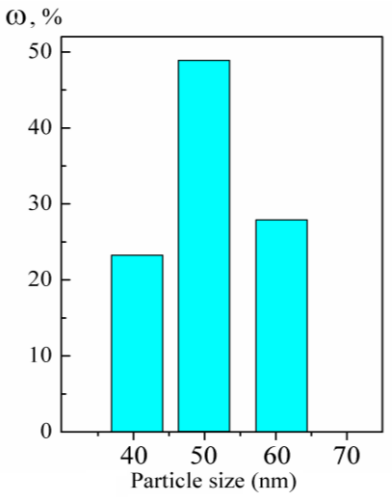

Fig. 3 – Particles size distribution of Al_2O_3

DTA curve of the as-prepared Al_2O_3 sample revealed a strong exothermic effect in the range 1200-1400 °C with a maximum at 1296 °C (see Fig. 4), which corresponds to the metastable alumina phase→α-Al_2O_3 phase transition [10]. This phase transformation has been extensively studied, and at present, it is well known that α-Al_2O_3 is formed through a nucleation and growth process, and depending upon chemical prehistory of the precursor, degree of its crystallinity, the presence of impurities etc. the transition temperature varies from 950 to 1350 °C [10].

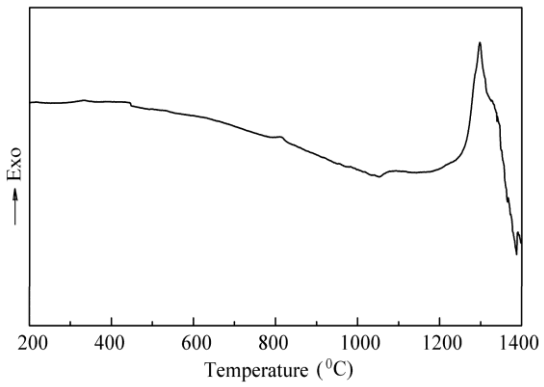

Fig. 4 – DTA curve of nanosized Al_2O_3

The second step in the preparation involved the formation of mixed rare earth oxides Tb_4O_7:Ce. To this end, the appropriate amounts of Tb_4O_7 (99.99 %) and CeO_2 (99.99 %) were dissolved in a dilute HNO_3 solution.

The hydrous mixed rare earth oxalates $R_2(C_2O_4)_3 \cdot nH_2O$ were precipitated from the hot solution (80 °C) by the slow addition of a concentrated $H_2C_2O_4$ solution. The precipitates were filtered, washed with distilled water, dried and then heated at 850 °C for 1 h in air. It is known that oxalate precursor-derived rare earth oxides typically consist of submicron aggregates of nanosized crystals [11]. After that the calculated amounts of Tb_4O_7:Ce and Al_2O_3 were grinded and thoroughly mixed in ethanol, and the resulting mixtures were fired at a temperature of about 1300 °C for 3-5 h in a reducing medium created by burning activated carbon.

The XRD patterns of the as-prepared samples were well matched with JCPDS File No. 76-0111 for TAG. The synthesis procedure used was not further optimized for emission intensity or particle size distribution, but even without this highly efficient luminescent materials were obtained.

The emission and excitation spectra of undoped $Tb_3Al_5O_{12}$ at 293 K are presented in Fig. 5. The emission spectrum contains several groups of bands in the range 470-640 nm, which are caused by the $^5D_4 \rightarrow {}^7F_j$ (j = 3-6) transitions of Tb^{3+} ions. The emission from the higher-energy $^5D_3$ state is practically absent due to the cross-relaxation process ($^5D_3 \rightarrow {}^5D_4$) : ($^7F_6 \rightarrow {}^7F_0$). The excitation spectrum of the emission consists of several intense and overlapping bands in the 250-300 nm region, a band of lower intensity at 325 nm and a number of relatively narrow bands at the longer wavelengths. It is evident that the broad bands are caused by the Tb^{3+} $4f^8 \rightarrow 4f^75d$ transitions, while the narrow ones are due to the $4f^8 \rightarrow 4f^8$ transitions of Tb^{3+} ions [4-6].

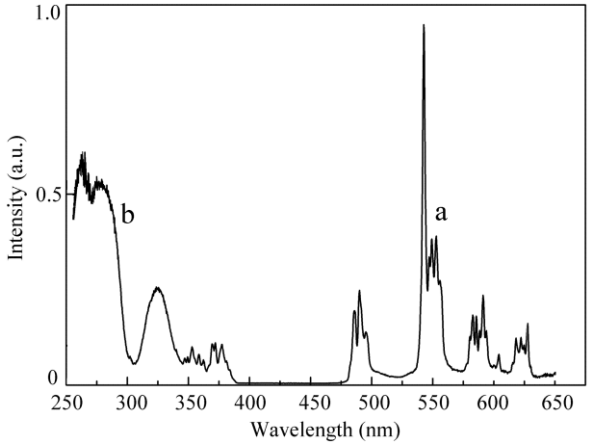

Fig. 5 – Emission and excitation spectra of $Tb_3Al_5O_{12}$ at 293 K. The emission spectrum (a) was recorded upon excitation at 370 nm and the excitation spectrum (b) was recorded for the Tb^{3+} emission at 540 nm

The emission spectra of TAG:Ce^{3+} depend on cerium concentration and excitation wavelength. As can be seen from Fig. 6, upon excitation at 450 nm the emission band of $Tb_{3(1-x)}Ce_{3x}Al_5O_{12}$ (x = 0.03) extends from 480 to 750 nm and has a maximum at about 563 nm. At 77 K the spectrum shows the doublet structure and can be reasonably decomposed into Gaussian-type bands with maxima at 534 and 583 nm, which are due to transitions from the lowest Ce^{3+} 5d excited state to the 4f ground state levels $^2F_{5/2}$ and $^2F_{7/2}$.

The positions of these maxima are in agreement with the results reported for the Ce^{3+} emission in TAG at 10 K [3]. The excitation spectrum of $Tb_{3(1-x)}Ce_{3x}Al_5O_{12}$ (x = 0.03) recorded for the Ce^{3+} emission at 560 nm is also shown in Fig. 6. No doubt that the broad band with a maximum at 465 nm is mainly caused by the 4f → 5d transition to the lowest component of the Ce^{3+} 5d configuration, while the narrow ones are due to the $4f^8 \rightarrow 4f^8$ transitions of Tb^{3+} ions. The band at 334 nm is a superposition of bands with maxima at 325 and 338 nm arising from spin-forbidden $4f^8 \rightarrow 4f^75d$ transition of Tb^{3+} ions and 4f → 5d transition of Ce^{3+} ions, respectively, so that its shape and relative intensity

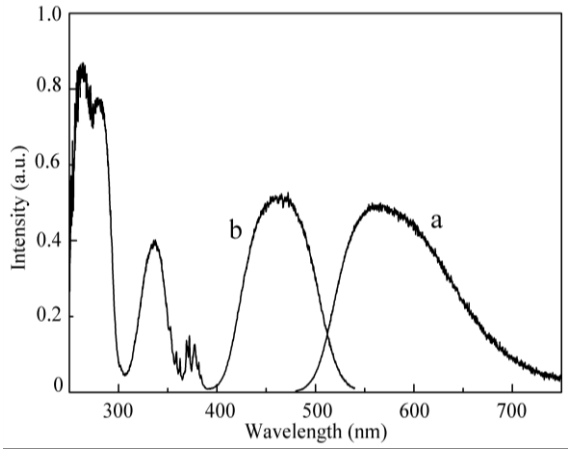

Fig. 6 – Emission and excitation spectra of $Tb_{3(1-x)}Ce_{3x}Al_5O_{12}$ (x = 0.03) at 293 K. The emission spectrum (a) was recoded upon excitation at 450 nm and the excitation spectrum (b) was recorded for the Ce^{3+} emission at 560 nm

depend on the emission wavelength and temperature. The spectrum also contains overlapping bands with maxima at 277 and 262 nm, which were also present in the excitation spectrum for the Tb^{3+} emission in TAG (see Fig. 5). It is clear that these bands must be attributed to the $4f^8 \rightarrow 4f^75d$ transitions of the Tb^{3+} ions [5]. The substitution of Tb^{3+} for Y^{3+} in the garnet structure results in broadening the emission band and shifting its maximum towards the longer wavelengths. At room temperature the full width at half maximum of the Ce^{3+} emission increases from 3460 cm^{-1} (YAG) to ~ 3800 cm^{-1} for TAG. When the larger Tb^{3+} ion occupies the Y^{3+} position, the dodecahedral site is expanded and distorted, so that these results can be explained by an increase in both the crystal field splitting of the Ce^{3+} 5d configuration and Stokes shift of the emission. Indeed, because the lowest Ce^{3+} excitation band of $Tb_{3(1-x)}Ce_{3x}Al_5O_{12}$ (x = 0.03) is situated at 465 nm (Fig. 6), the Stokes shift of the emission amounts to 2780 cm^{-1}. This value is somewhat larger than that reported for the Ce^{3+} emission in YAG (2400 cm^{-1}) [12]. The quantum efficiency of luminescence (η) of the $Tb_{3(1-x)}Ce_{3x}Al_5O_{12}$ (x = 0.03) sample was determined as described in Refs. [1, 2] using a commercial YAG: Ce^{3+} phosphor for LED's with η = 0.90 as a standard.

For the excitation at 460 nm, the found value of 0.83 ± 0.04 is comparable to, but somewhat larger than that (η = 0.76) reported in the literature for the Ce^{3+} emission in TAG prepared at 1500 °C [4].

4. CONCLUSIONS

TAG:Ce^{3+} phosphor has been successfully prepared with the use of nanostructured oxides of aluminum and rare earths. Spherical Al_2O_3-particles with a diameter ranging from 20 nm to 70 nm were obtained by gaseous-disperse synthesis. It was shown that the Ce^{3+} ions in TAG exhibit the intense broad band emission with a maximum at about 563 nm and the quantum efficiency of luminescence of the $Tb_{3(1-x)}Ce_{3x}Al_5O_{12}$ (x = 0.03) phosphor was found as high as 0.83.

Люмінесцентні властивості активованих Ce^{3+} тербій-алюмінієвих гранатів, синтезованих з використанням наноструктурованих реагентів

І.В. Березовська[1], Б.І. Заднепровський[2], М.І. Полетаєв[3], Ю.А. Дорошенко[3], Н.П. Єфрюшина[1], О.В. Зубар[1], В.П. Доценко[1]

[1] *Фізико-хімічний інститут ім. О.В. Богатського НАН України, Люстдорфська дорога, 86, 65080 Одеса, Україна*
[2] *Центральний науково-дослідницький інститут хімії та механіки, 115487 Москва, Росія*
[3] *Інститут горіння та нетрадиційних технологій, Одеський Національний університет ім. І.І. Мечнікова, вул. Дворянська, 2, 65082 Одеса, Україна*

У статті описується синтез активованого іонами Ce^{3+} тербій-алюмінієвого гранату (TAG) з використанням наноструктурованих оксидів рідкісноземельних елементів та алюмінію. Наночастки Al_2O_3 були одержані за допомогою газодісперсного синтезу та охарактеризовані методами рентгенівської дифракції, диференційно-термічного аналізу та електронної скануючої мікроскопії. Встановлено, що іони Ce^{3+} в TAG демонструють інтенсивну широкосмугову люмінесценцію з максимумом при 563 нм та квантова ефективність люмінесценції матеріалу складу $Tb_{3(1-x)}Ce_{3x}Al_5O_{12}$ (x = 0.03) досягає 0.83.

Ключові слова: Тербій Алюмінієвий Гранат, Синтез, Наночастки, Люмінесценція.

Люминесцентные свойства активированных Ce^{3+} тербий-алюминиевых гранатов, синтезированных с использованием наноструктурированных реагентов

И.В. Березовская[1], Б.И. Заднепровский[2], Н.И. Полетаев[3], Ю.А. Дорошенко[3], Н.П. Ефрюшина[1], Е.В. Зубарь[1], В.П. Доценко[1]

[1] *Физико-химический институт им. А.В. Богатского НАН Украины, Люстдорфская дорога, 86, 65080 Одесса, Украина*
[2] *Центральный научно- исследовательский институт химии и механики, 115487 Москва, Россия*
[3] *Институт горения и нетрадиционных технологий, Одесский Национальный университет им. И.И. Мечникова, ул. Дворянская, 2, 65082 Одесса, Украина*

В статье описывается синтез активированного ионами Ce^{3+} тербий-алюминиевого граната (TAG) с использованием наноструктурированных оксидов редкоземельных элементов и алюминия. Наночастицы Al_2O_3, полученные с помощью газодисперсного синтеза, были охарактеризованы методами рентгеновской дифракции, дифференциально-термического анализа и сканирующей электронной микроскопии. Установлено, что ионы Ce^{3+} в TAG обладают интенсивной широкополосной люминесценцией с максимумом при 563 нм и квантовая эффективность люминесценции материала состава $Tb_{3(1-x)}Ce_{3x}Al_5O_{12}$ (x = 0.03) достигает 0.83.

Ключевые слова: Тербий Алюминиевый Гранат, Синтез, Наночастицы, Люминесценция.

REFERENCES

1. A.A. Setlur, W.J. Heward, Y. Gao, A.M. Srivastava, R.G. Chandran, M.V. Shankar, *Chem. Mater.* **18**, 3314 (2006).
2. A. Katelnikovas, H. Bettentrup, D. Uhlich, S. Sakirzanovas, T. Justel, A. Kareiva, *J. Lumin.* **129**, 1356 (2009).
3. H.S. Jang, W.B. Im, D.C. Lee, D.Y. Jeon, S.S. Kim, *J. Lumin.* **126**, 371 (2007).
4. M. Nazarov, D.Y. Noh, J. Sohn, C. Yoon, *J. Solid State Chem.* **180**, 2493 (2007).
5. Y. Zorenko, V. Gorbenko, T. Voznyak, M. Batenschuk, A. Osvet, A. Winnacker, *J. Lumin.* **128**, 652 (2008).
6. K.M. Kim, J.H. Ryu, S.W. Mhin, G.S. Park, K.B. Shim, *J. Electrochem Soc.* **155**, J293 (2008).
7. J.D. Furman, G. Gundiah, R. Rage, N. Pizarro, A.K. Cheetham, *Chem. Phys. Lett.* **465**, 67 (2008).
8. W. Zhao, S. Anhel, C. Mancini, D. Adams, G. Boulon, T. Epicier, Y. Shi, X.Q. Feng, Y.B. Pan, V. Chani, A. Yoshikawa, *Opt. Mater.* **33**, 684 (2011).
9. N.I. Poletaev, A.N. Zolotko, Yu.A. Doroshenko, *Combust. Expl. Shock* **47**, 153 (2011).
10. P.-L. Chang, F.-S. Yen, K.-C. Cheng, H.-L. Wen, *Nano Lett.* **1**, 253 (2001).
11. A.A. Titov, M.A. Klimenko, E.G. Goryacheva, N.L. Opolchenova, N.N. Stepareva, N.P. Sokolova, *Inorgan. Mater.* **44**, 1101 (2008).
12. V. Bachmann, C. Ronda, A. Meijerink, *Chem. Mater.* **21**, 2077 (2009).